Preclinical characterization of a potential best-in-class camptothecin-based antibody-drug conjugate targeting ADAM metallopeptidase domain 9

Poster Section 11, Board #26
Published Abstract #4418

Rui Liu, Lan Ding, Yushi Chi, Ge Song, Kuichao Qu, Wan-jen Yang, Kun Yan, Jinbo Liu, Huixin Yan, Xiaoling Yuan, Ying Chen, Zhenjian Li, Chen Hu, Jijun Yuan
Shanghai Henlius Biotech, Inc., Shanghai, China

Background:

ADAM metallopeptidase domain 9 (ADAM9) is a member of the disintegrin and metalloproteinase, mediates proteolytic shedding of cytokines and growth factors. ADAM9 dysregulation promotes tumor progression, metastasis, and pathological angiogenesis. ADAM9 is overexpressed in various solid tumors, including pancreatic, lung, gastric, and breast cancers, with low expression in normal adult tissues. Previously, the clinical development of ADAM9-targeted ADC IMGC-936 was terminated due to maytansinoid-related ocular toxicities. Herein, we developed a next-generation ADAM9 ADC using a camptothecin-based linker-payload, which is anticipated to avoid ocular toxicity and possess expanded therapeutic index.

Methods:

ADC cytotoxicity was evaluated using the CellTiter-Glo (CTG) assay in Jurkat (ADAM9-negative), Calu-3 (intermediate ADAM9 expression), and NCI-H1693 (high ADAM9 expression) cell lines. Bystander activity was assessed in Jurkat cells co-cultured with CHOK1-hADAM9 cells, with Jurkat viability determined by CTG. ADC stability in human and rat plasma was monitored over 14 days, with payload release quantified by LC-MS. Accelerated stability was examined by incubating ADCs at 25 °C for 7 days, followed by drug antibody ratio (DAR) and size exclusion chromatography monomer fraction analysis. In vivo efficacy was investigated in Calu-3 (non-squamous NSCLC, EGFR wildtype) and DLD-1 (CRC, MSI-H, KRAS G13D) cell line-derived xenograft (CDX) mouse models. A PK study was conducted in Sprague-Dawley rats administered intravenously with ADAM9 ADC 5 mg/kg.

Results:

The parental antibody exhibited nanomolar affinity for human and cynomolgus ADAM9, with no cross-reactivity to rodent orthologs or other ADAM family members. Compared to the benchmark, the anti-ADAM9 antibody demonstrated superior internalization capability in Miapaca-2 cell, while the ADC showed comparable or enhanced internalization in CHOK1-hADAM9 cell. The ADAM9-ADC demonstrated potent cytotoxicity and bystander killing effects. In Calu-3 CDX models, a single 3 mg/kg dose elicited 109.3% tumor growth inhibition (benchmark ADC, 91.1%). In DLD-1 CDX models, TGIs reached 66.8% and 90.2% at 3 and 8 mg/kg, respectively, significantly outperforming the benchmark (39.2%) at 3mg/kg. The ADC also displayed excellent plasma stability, with minimal DAR reduction and aggregation in accelerated and freeze-thaw stability assays. The ADAM9 ADC also exhibited a favorable pharmacokinetic profile in rats, characterized by minimal free toxin release and antibody-like half-life.

Conclusions:

Preclinical studies demonstrated that the ADAM9-ADC exhibits potent *in vitro* cytotoxicity and superior *in vivo* antitumor efficacy relative to benchmarks. Pilot toxicology studies in cynomolgus monkeys are ongoing.

Key Design Features of the ADAM9 ADC

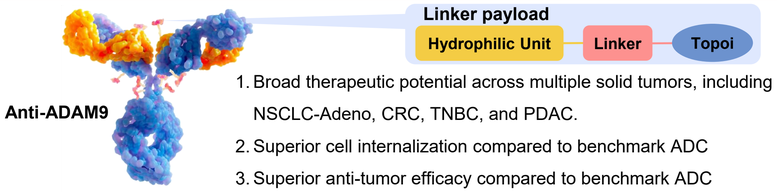

1. Broad therapeutic potential across multiple solid tumors, including NSCLC-Adeno, CRC, TNBC, and PDAC.
2. Superior cell internalization compared to benchmark ADC
3. Superior anti-tumor efficacy compared to benchmark ADC

In Vitro Binding Properties of Anti-ADAM9 Antibody and ADC

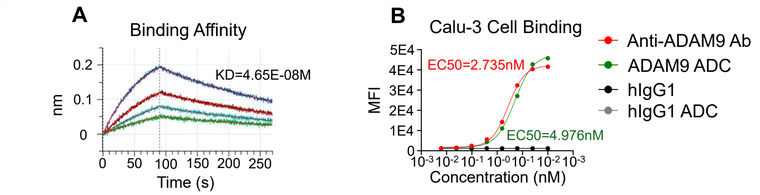

Figure 3. Binding affinity of the anti-ADAM9 antibody to the ADAM9 extracellular domain was determined by biolayer interferometry (BLI) (A). Cell binding of the anti-ADAM9 antibody and corresponding ADC to ADAM9⁺ Calu-3 cells was assessed by flow cytometry (B).

Efficient Internalization of Anti-ADAM9 Antibody and ADC

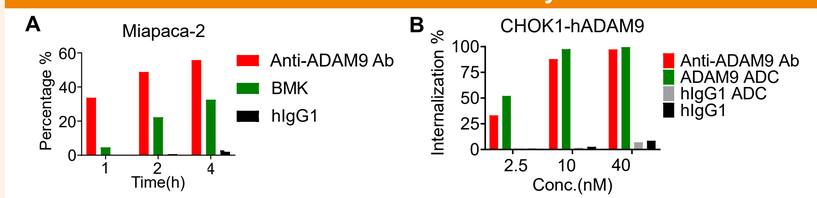

Figure 2. Time-dependent internalization of the anti-ADAM9 antibody was compared with a benchmark antibody (BMK) in Miapaca-2 cells using a pHrodo-based assay (A). Concentration-dependent internalization of the anti-ADAM9 antibody and corresponding ADC was assessed in CHO-K1-hADAM9 cells at 2.5, 10, and 40 nM (B).

ADAM9 ADC Exhibits Target-Expression-Dependent *In Vitro* Cytotoxicity

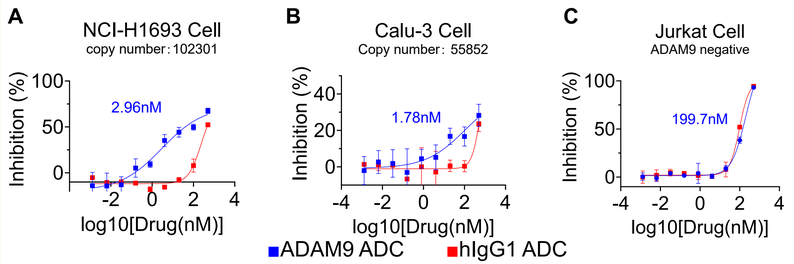

Figure 4. *In vitro* cytotoxic activity of the ADAM9 ADC in cell lines with different levels of ADAM9 expression, including NCI-H1693 (A), Calu-3 (B), and Jurkat (C). The approximate cell-surface ADAM9 copy numbers, as reported in the literature, are indicated at the top of each panel. Cells were incubated with serially titrated concentrations of the indicated ADCs for 96 hours, and cell viability was assessed by CTG assay.

ADAM9 ADC Exhibits Potent Bystander Killing Activity

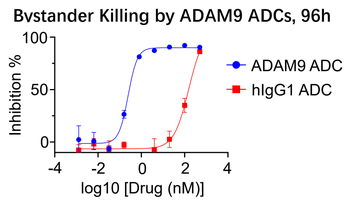

	Rel. IC_{50} (nM)	I_{max} %
ADAM9 ADC	0.25	92.58
hIgG1 ADC	156.4	107.8

Figure 5. Bystander killing activity was evaluated in Jurkat cells co-cultured with CHOK1-hADAM9 cells and treated with the indicated ADCs for 96 hours. Jurkat cell viability was quantified using the CTG assay.

ADAM9 ADC Exhibits Excellent Plasma and Thermal Stability

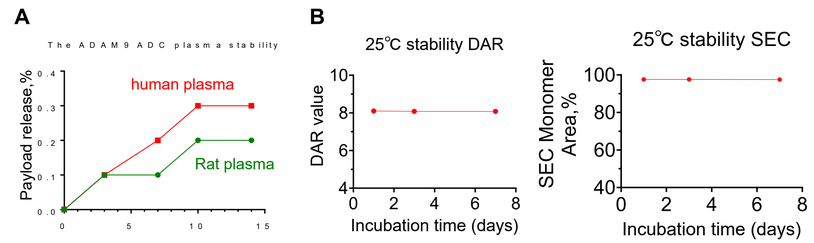

Figure 8. The Plasma stability & Pre-CMC stability analysis of ADAM9 ADC. The free payloads (A) in Rat and human plasma were measured by LC-MS/MS, the DAR values (B) were measured by LC-MS/MS and the SECs (B) were measured by HPLC.

ADAM9 ADC Exhibits Superior *In Vivo* Antitumor Efficacy Compared with the Benchmark in Two CDX Models

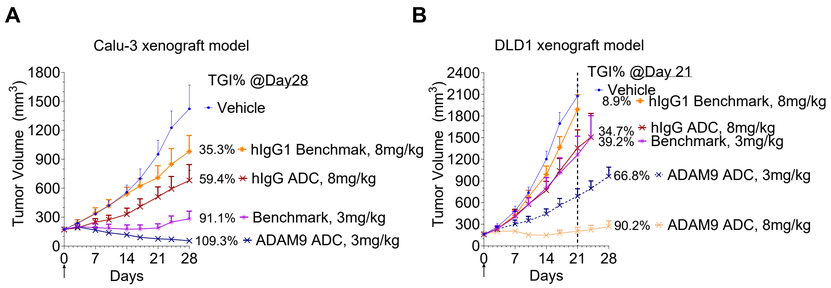

Figure 6. (A) Calu-3 cells, non-sqNSCLC (EGFR WT), were implanted subcutaneously into 6–8-week-old BALB/c nude mice, and treatment was initiated when tumor volume reached ~190 mm³. (B) DLD1 CRC cells, which harbors the MSI-H and KRAS G13D mutation, were established in BALB/c nude female mice and dosing began at a volume of ~170 mm³. All ADCs were DAR 8. n=6 for each group.

ADAM9 ADC Exhibits Favorable Pharmacokinetic Properties in Sprague-Dawley Rats

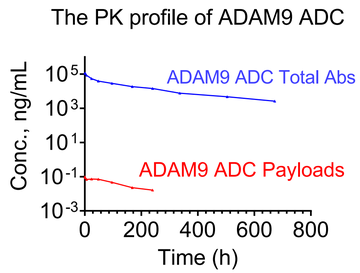

PK parameters		Total Abs	toxin
$t_{1/2}$	(h)	210	/
C_{max}	(ng/mL)	111746.54	0.1
AUC_{last}	(h*ng/mL)	10156081.34	10.2
AUC_{0-inf}	(h*ng/mL)	10940718.56	12.6
Cl	(mL/h/kg)	0.46	/
MRT_{0-inf}	(h)	221	/
Vss	(mL/kg)	101.2	/

Figure 7. Pharmacokinetic profiles of total antibody and free payload following intravenous administration of ADAM9 ADC in Sprague-Dawley rats. DAR value = 8.

Disclosures: RL, LD, YC, GS, KQ, WY, KY, JL, HY, XY, YC, ZL, CH, JY are employees of Henlius.

Email: Rui_Liu1@henlius.com